Accepted Manuscript

Preparation and comparison of spray dried and electrospun bioresorbable drug delivery systems

Péter L. Sóti, Zsombor K. Nagy, Geert Serneels, Balázs Vajna, Attila Farkas, Filip Van der Gucht, Pál Fekete, Tamás Vigh, István Wagner, Attila Balogh, Hajnalka Pataki, Gábor Mező, György Marosi

PII: S0014-3057(15)00170-6
DOI: http://dx.doi.org/10.1016/j.eurpolymj.2015.03.035
Reference: EPJ 6825

To appear in: *European Polymer Journal*

Received Date: 29 September 2014
Revised Date: 7 March 2015
Accepted Date: 16 March 2015

Please cite this article as: Sóti, P.L., Nagy, Z.K., Serneels, G., Vajna, B., Farkas, A., Gucht, F.V.d., Fekete, P., Vigh, T., Wagner, I., Balogh, A., Pataki, H., Mező, G., Marosi, G., Preparation and comparison of spray dried and electrospun bioresorbable drug delivery systems, *European Polymer Journal* (2015), doi: http://dx.doi.org/10.1016/j.eurpolymj.2015.03.035

Preparation and comparison of spray dried and electrospun bioresorbable drug delivery systems

Péter L. Sóti[a], Zsombor K. Nagy[a], Geert Serneels[b], Balázs Vajna[a], Attila Farkas[a], Filip Van der Gucht[b], Pál Fekete[a,c], Tamás Vigh[a], István Wagner[a], Attila Balogh[a], Hajnalka Pataki[a], Gábor Mező[d], György Marosi[a]*

[a] Department of Organic Chemistry and Technology, Budapest University of Technology and Economics, H-1111 Budapest, Műegyetem rkp. 3-9, Hungary

[b] Pro-C-epT Ltd., 9060 Zelzate, Industriepark Rosteyne 4, Belgium

[c] Meditop Pharmaceutical Ltd., H-2097 Pilisborosjenő, Ady Endre utca 1, Hungary

[d] Research Group of Peptide Chemistry, Hungarian Academy of Sciences, Eötvös Loránd University, H-1117 Budapest, Pázmány Péter sétány 1/A, Hungary

---

* Corresponding author at: Department of Organic Chemistry and Technology, Budapest University of Technology and Economics, Műegyetem rkp. 3-9, H-1111 Budapest, Hungary. Tel.: +36 1 4633654; fax: +36 1 463 3648. E-mail address: gmarosi@mail.bme.hu (G. Marosi).

Abstract

Two continuous processes, the spray drying method, producing microparticles in presence of hot gas flow, and the electrospinning technology, producing continuous polymer nanofibers at low temperature under high electric fields, were investigated and compared the first time. Both techniques were used to prepare slow release caffeine (as a model of rapidly water-soluble drug) using water-insoluble, biocompatible and bioresorbable PLGA and PLA as polymeric matrix. The structural characterization of the obtained samples was performed using SEM, XRD, DSC and at-line Raman mapping, while in vitro dissolution was detected by UV spectrophotometer. We found that the release profile of a highly water soluble drug can be adjusted to the requirements through the investigated continuous technologies. Solid molecular dispersion of caffeine at colloidal level could be prepared in PLA matrix using electrostatic spinning. Furthermore the continuous nonwoven structure of ultrafine fibers, produced this way, allows easer handling than that of independent fine particle's. On the other hand continuous production of drug loaded microspheres with slightly less performance can be performed with the conventional technology of spray drying which is well known in the pharmaceutical industry.

Keywords:

Electrospinning, Spray drying, Biopolymer, Sustained release, Chemometrics

1. Introduction

The control of drug release poses great challenges for the pharmaceutical industry regardless of poor or high solubility of the active pharmaceutical ingredient (API) in water. In the case of highly water-soluble active drugs, which are otherwise rapidly eliminated from the body, the requirement is to find the appropriate technology and excipients to achieve smooth and sustained drug release. The methods assigned for this purpose should be gentle and productive enough allowing efficient manufacturing on industrial scale. Although both the well-known spray drying (SD) and the recently introduced electrospinning (ES) techniques have been already used for forming controlled release formulations [1-5], these were, surprisingly, not yet tested with the same formulation comparing their capability.

Several investigations have revealed the suitability of SD for producing bioresorbable drug delivery systems in a continuous manner [6-8], providing the amorphous form of the APIs (in most cases). More recently, similar reports have appeared regarding ES [9-11]. The high tendency for amorphization in the cases of ES and SD is ascribed to the fast evaporation of the solvent [12], which results in amorphous solid dispersion or solution of the drug in the polymer matrix [9]. Amorphous state of a drug promotes its dissolution advantageously comparing to the crystalline state if it is stabilized by the surrounding polymer phase. is a disadvantage, however, that the SD technique requires elevated temperature that can damage thermally unstable compounds [13].

In order to achieve controlled release of drugs of high water solubility with these techniques, the selected polymer matrices must not be (or just very slowly) soluble in water allowing smooth release of drug. Poly(lactic acid) (PLA) and poly(lactide-co-glycolide) (PLGA) are such

bioresorbable and thermoplastic water-insoluble polymers (approved by all the relevant authorities for use in human subjects). These biocompatible polymers have been employed as suture materials [8], inter-body cages [14], scaffolds for tissue engineering [15], and biodegradable drug delivery systems [16] with sustained drug release [17]. Both PLA and PLGA matrices are frequently applied to achieve sustained drug release , but a so-called "burst effect" is experienced in many cases [18, 19]. Significant initial burst release can result in such a high drug concentration in the blood that means significant risk to the patient's health. Furthermore, early depletion of the drug in these cases is a further disadvantage regarding the intended long-term release. Currently, burst release values between 10% and 80%, depending on the encapsulated drug load, are commonly seen in publications as well as in marketed products [20].

The objective of this study was to prepare sustained-release caffeine (as a model of water-soluble API) by spray drying and electrospinning and evaluate the capabilities of these methods for amorphization and controlled release by solid-phase analytical methods and in vitro dissolution tests.

2. Experimental

2.1 Materials

The poly(lactide-co-glycolide) (PLGA) block copolymer used in this work was PURASORB® PDLG 5004, M_w = 40,000, inherent viscosity of 0.4 dl/g (25 °C), it contains 50 % D,L-lactide. Polylactic acid homopolymer was PURASORB® PL 24 (PLA, D isomer < 5 %) (both obtained from PURAC; Netherlands). Caffeine was purchased from Sigma-Aldrich Chemie GmbH (Germany). Dichloromethane (CH_2Cl_2); chloroform ($CHCl_3$) and N, N-dimethylformamide (DMF) was obtained from Reanal Private Ltd. (Hungary).

Figure 1

2.2 Spray drying and electrospinning processes

Microspheres with and without caffeine were prepared using spray drying method. For this purpose, PLGA of 5 % (w/v) and PLA of 1 % (w/v) concentrations, respectively, were dissolved in CH_2Cl_2 and caffeine was added in different concentrations (0-100 w/w%) to the solution of the polymers. The code and concentration of samples prepared are given in Table 1. Spray-drying was performed with a Pro-Cep-T 4M8-TriX spray dryer (ProCept, Belgium) using a 0.4 mm two-fluid nozzle. The process parameters were as follows: atomization air pressure 1 bar; inlet air temperature 40 °C; outlet air temperature 38 °C; pump control 2.24 mL/min; airflow 0.8 m^3 min^{-1}.

Table 1

Electrospun fibers were prepared using and 4, 6 and 10 (w/w %) PLA solution in $CHCl_3$: DMF = 6:1 co-solvent system to which 0, 10, 20 or 50 (w/w) % caffeine was added. All electrospinning experiments were performed at room temperature (24 ± 2 °C) assembling the fibers on aluminum foil affixed to the collector. To perform electrospinning, an infusion pump (Aitecs SEP-10S Plus syringe pump, Lithuania) and constant voltage ranging from 20–30 kV were applied provided by a direct current power supplier (NT-35 High Voltage DC Supply MA2000, Hungary). The distance between the collector and the spinneret (with 0.4 mm internal diameter) was 23 cm and the solutions were fed with 0.13 mL/min rate.

The yields were determined based on outcome of the solid product related to the solid starting materials.

2.3 At-line Raman spectrometry and mapping

At line measurements were performed using a LabRAM 300 micro-Raman spectrometer manufactured by Jobin Yvon Horiba (France) and equipped with a fiber optic coupled probe,

using a 400 mW, 785 nm laser source and an air cooled CCD detector. The instrument is described elsewhere [21]. All spectra were detected over the range of 500–1800 cm^{-1} approximately 4 cm^{-1} resolution provided by a grating monochromator of 950 groove/mm. In each experiment the acquisition time was 0.5 s and 80 spectra were averaged. Each sample was measured at 25 different point of the surface (spectra from different locations were not averaged).

Chemical mapping was carried out on selected electrospun and spray-dried samples using above mentioned micro-Raman spectrometer to obtain information on their API distribution. In these cases, an external laser source of 532 nm frequency-doubled Nd-YAG was used. The spectra were recorded on the spectral range of 400-1835 cm^{-1}. The high resolution maps were collected with an objective of ×100 magnification (laser spot size: ~0.7 μm) and 1 μm step size. The acquired image consisted of 41 × 41 points (pixels). Each single spectrum was acquired for 5-7 s and 5 or 8 spectra were averaged in each pixel depending on the available measurement time.

2.4 Data analysis of Raman spectra

Before chemometric evaluation, piece-wise linear base-line correction was applied on all spectra (using the same baseline points for all the maps and reference spectra). Afterwards, spectra were normalized to unit area. Concentrations of the ingredients in the samples were computed using Partial Least Squares (PLS) regression. A PLS model was built on a calibration set consisting of multiple spray-dried samples with various concentration levels (Table 1). The details of PLS can be found in the literature [22]. The number of latent variables was set to 2 as the samples consisted of 2 components (and all subsequent latent variables (loadings) contained mostly noise and instrumental disturbance factors that did not hold valuable chemical

information). Best results were obtained when mean centering was also applied on the calibration and prediction sets as a third preprocessing step.

The efficiency of the calibration and validation model was calculated using the root mean square error of calibration (RMSEC), cross-validation (RMSECV), and prediction (RMSEP). Besides, the corresponding coefficients of determination (R2) were calculated as well. For RMSECV, a contiguous block cross-validation was performed: in each step, a contiguous block of spectra of the calibration set was deleted from the calibration set and a model was built with the remaining spectra. The errors were calculated based on the samples left out and the procedure was repeated with leaving out the next block of spectra in the calibration matrix. In practice, this approach means leaving out all spectra for a particular concentration at a time.

$$RMSE = \sqrt{\frac{\sum_{i=1}^{N}(y_i - \bar{y}_i)^2}{N}}$$

Equation 1 Root mean square error calculation

All calculations were performed in MATLAB 7.6.0 (Mathworks, USA) with PLS_Toolbox 6.0.1 and MIA_Toolbox 2.0.1 (Eigenvector Research, USA).

2.5 Scanning electron microscopy (SEM) and polarized microscopy (PM)

The surface morphology of the microparticles and submicron-sized fibers were investigated by a JEOL JSM 6380LA (Tokyo, Japan) scanning electron microscope (acceleration voltage: 10–30 kV) and an Amplival Carl Zeiss (Jena, Germany) polarized microscope (PM). The images were collected with OLYMPUS C4040 Z type camera, the evaluation was performed with the aid of DP-Soft software. Samples for SEM were dried under vacuum, mounted on metal stubs, and sputter-coated with gold/silver binary alloy.

2.6 X-ray diffractometry (XRD)

The pure caffeine, PLGA, PLA and caffeine-loaded biodegradable microspheres and fibers were analyzed with a PANalytical X'pert Pro X-ray MPD diffractometer (Almelo, The Netherlands). The measurements were under CuK_{α} (λ=1.5406 Å), 40 kV and 30 mA as X-ray source with Kb (Ni) filter. The diffraction patterns were collected with 2θ ranging from 2 or 4 ° to 42°.

2.7 Differential scanning calorimetry (DSC)

Thermal analyses of all the above-mentioned samples were carried out using SETARAM DSC 92 (Calure, France). 10 – 20 mg sample was in an aluminum pan. An empty aluminium pan was used as reference. The measurements were carried out in 1.6 bar nitrogen atmosphere. The heating rate was 10 °Cmin^{-1}. The heating scans were performed from 30 to 300 °C.

2.8 In vitro release studies of caffeine

In vitro drug dissolution tests were performed in 900 mL at 37±1 °C tempered distilled water by Erweka DT6 dissolution tester (Erweka, Heusenstamm, Germany) with 50 min^{-1} stirring speed. Solid dispersions, contained about 10 mg API, were filled in spherical shape wire mesh and it was dipped in the dissolution bath in order to ensure the total surface wettability of the microparticles and fibers. 5 mL sample was taken at various intervals and its caffeine concentration was determined by UV spectrophotometry at 274 nm (Hewlett-Packard - HP 8452A Diode Array UV/VIS spectrophotometer).

3. Results and discussion

Spray drying and electrospinning technologies enable continuous production of the biodegradable drug delivery systems. Raman spectrometry, as non-destructive analytical method, is suitable for monitoring the structure and the API concentration assisting thus in optimizing the process parameters. In order to suppress the rapid release of drug from the matrices, numerous formulations were prepared in case of SD by varying also the polymer matrices (PLGA and PLA). Considering the results of screening performed by spray drying the electrospinning experiments were performed only with the most promising systems.

3.1 Preparation of spray dried and electrospun systems of various drug concentrations controlled by at line Raman spectrometry

The composition of the prepared samples and the yield of their production are given in Table 1. The code expresses the way of processing (spray drying: SD, electrospinning: ES), the polymer (polylactic acid: PLA, poly(lactide-co-glycolide): PLGA) and the composition as given in the table. The yields in the case of electrospinning were significantly better (94 - 97%) than in the case of spray drying (generally 50 - 80%) which can be explained by the high efficiency of the electrostatic particle collection. Furthermore, the continuous non-woven structure of the nanofibers allows much easier handling of the produced material (as a textile) than in the case of independent spray dried particles (fine powder).

Wide scope of the SD compositions, prepared by spray drying, served for evaluating the capability of the polymer matrices to control the release of caffeine. As the in vitro release results of PLGA, given in section 3.5, were not promising the electrospinning experiments were performed with PLA in the concentration range that is realistic for application. Nevertheless, all the prepared samples were subjected to structural analysis.

Raman spectrometry, as a potential PAT (process analytical technology) tool [23], was used, at the site of spray drying to check the caffeine concentration of the formed objects (ES samples were not analyzed this way as electrospinning process is not yet present in pharmaceutical industry). Figure 2 shows the spectra of the caffeine-PLGA samples.

Figure 2

The crystalline form of caffeine in the samples is represented by its sharp peaks. The two peaks of highest intensity at 1328 cm^{-1} (νC-N stretching vibrations [24]) and at 555 cm^{-1} (δO=C-N bending vibrations [25]) are characteristic to caffeine, the intensities of which grow along with its concentration in the sample. PLGA does not have any sharp peaks; there is only one significant peak at 1769 cm^{-1} (νC=O stretching vibrations) that diminishes as the concentration of PLGA decreases in the samples.

Figure 3

Raman spectra of PLA-caffeine mixtures in Figure 3 are also dominated by the same two bands characteristic of caffeine (1328 and 555 cm^{-1}) as in the previous series. Regarding the PLA matrix, the peak at 1769 cm^{-1} refers to the same functional group as in the case of PLGA, namely, the lactate unit. The intense peak at 872 cm^{-1} (νC-COO stretching vibrations [26]) is present only in samples containing PLA. In order to control the caffeine concentration in the samples effectively, the average Raman spectra of the compositions were evaluated using PLS regression method (considering the entire spectra, instead of selecting particular vibrational peaks. Preliminary studies showed that univariate calibration was not feasible due its high prediction error). The spectral dataset contained 11 different caffeine-PLGA and 6 caffeine-PLA samples with different mass fractions. (PLGA and PLA sets were evaluated separately.) These datasets were divided into two subsets in 6 : 5 and 4 : 2 ratio, respectively. One subset, called calibration set, was used to build the regression model. The other subset, called prediction set, was used to

predict the predictive performance of the model. The performance of the model was primarily evaluated based on the root mean square errors (RMSE), but the coefficients of determination (R2) were also calculated. The model plots are shown in Figure 4, while the numeric indicators of the regression performance are presented in Table 2.

Figure 4

Table 2

A small degree of nonlinearity was observed in the correspondence of the predicted versus the nominal concentration (Figure 4). This is due to the normalization applied. (However, normalization could not be avoided as it was required to remove the overall intensity deviations among pixels and doing so lead to much higher prediction errors, even though the correspondence between predicted and nominal concentrations stays almost completely linear.) As no outliers are seen on Figure 4, the results confirm that the composition of the formed samples did not change during processing and the PLS regression provides a robust model for controlling the concentration of API. This suggest: concentration of API can be examined in fast and precise manner by Raman spectrometry which is very useful in semi-continuous or continuous processing technologies.

3.2 Morphology and size of the microparticles and fibers

The morphology and average diameters of the particles were evaluated by SEM images.

Figure 5

As seen on Figure 5, the diameter of caffeine-loaded PLA microspheres was in the range of 3 – 10 μm. Shape of the spray dried PLA particles are spherical (Figure 5A), but as the caffeine concentration increases, the particles start losing their spherical shape: distorted and formless particles are obtained (Figure 5C, E). The solid dispersion loses its regular shape gradually, due to the increased caffeine content, forming various objects (including doughnut-like particles) in

the case of SD_PLA50 samples. These changes can indicate phase separation of the components and crystallization of caffeine in the particles.

The morphology of the ES fibers is shown in Figure 5B, D and F. The average diameter of the pure polymeric and caffeine-loaded fibers was determined using the SEM images. Table 3 summarizes the average diameters of fibers obtained from different compositions.

Table 3

A decrease of the fiber diameter with decreasing polymer concentration, enabling the preparation of submicron fibers, can be seen in Table 3. In contrast, inclusion of API into the PLA matrix increased the fiber diameter. Differences were observed in the surface appearance of the fibers as well: rough surface was characteristic to the sample containing 50% caffeine (suggesting phase separation), while the surface of fibers containing pure PLA and those with PLA and 10% caffeine were smooth (suggesting no phase separation). In order to determine the reason of the difference, polarized microscopic (PM) analyses were performed as well. The images taken by a polarized light optical microscope are shown in Figure 6.

Figure 6

The different appearance of the PLA fibers with 10% and 50% caffeine loading can be also recognized in the PM images. The colorful birefringent spots in the fiber of 50% caffeine content refer to crystalline parts grown inside the fibers, while the sample with less caffeine loading seems to be free of crystalline content. It was therefore assumed that in the ES_PLA10 sample the caffeine can be molecularly dispersed. This assumption was further investigated by other analytical methods.

3.3 DSC results

The aim of the thermal analysis was the determination of the morphology of the API. At first, pure caffeine and the pure polymers were analyzed. Sharp melting endotherms, characteristic to the crystalline materials, were visible in DSC curves of caffeine and PLA. In the case of PLGA glass transition was observable around 60 °C (Figure 8A). The phase transformation (from Form II to Form I) and melting point of caffeine Form II appears at 145 °C and at 234 - 239 °C (Figure 7B) respectively in accordance with the literature [27]. The enthalpy of the endothermic peak of caffeine melting in PLGA SD samples rapidly decreases with the concentration and below 10% drug content crystalline drug parts is negligible (Figure 8 and Figure 9). Similarly, within the SD PLA matrix the sign of the endothermic melting transition of caffeine disappears between 10-20% of drug content (Figure 9). Among the DSC curves (Figure 7) of ES fibers, the one for the ES_PLA10 sample (of 10% of caffeine content, curve "F") also suggests perfectly dispersed caffeine in the matrix as its separate melting peak cannot be detected.

Figure 7

Figure 8

Figure 9

Regarding the polymer phase characteristics, enthalpy change can be seen in the 60 - 80 °C regions of the curves in Figures 7 (C, D, E, F, G and H). This region includes the glass transition followed by increased segmental motion and "cold" crystallization in the course of the heating-up process as a consequence of the fast drying applied in the process: The time available for segmental arrangement in the course of SD and ES drying processes is not enough for crystallization of PLA therefore it becomes complete only when the temperature is raised above the glass transition temperature (Tg). The DSC curve of original PLA (see in Figure 7A) does not show such transition.

3.4 XRD

Changes of crystallinity induced by the manufacturing processes also were evaluated by X-ray diffraction measurements. The results are given in Figure 10 and Figure 11. According to the diffractograms spray drying resulted in amorphization only at 5% drug content. This result suggests that the DSC analysis alone is not suitable for evaluating the morphology of solid dispersions. Comparison of SD and ES techniques in the case of systems prepared with PLA matrix made clear that amorphization of drug at 10% caffeine concentration is only successful if ES is applied. The difference is probably caused by the different rates of solvent evaporation in the two methods. The SD produces particles of smaller specific surface releasing solvent less readily than the thin fibers formed by ES technique. The lower drying rate and the higher temperature of SD process provide sufficient time and mobility for nucleation of a readily crystallizing API (such as caffeine). In contrast, the drying and solidification processes are extremely rapid when fibers of large specific surface area is formed by ES method [1], furthermore, the diffusion, required for nucleation, is limited in the formed fibers owing to the partially oriented polymer chains and the excellent diffusion barrier properties of the fiber-air interfaces. Thus, even strongly crystallizing active substances can be kept in amorphous form.

Figure 10

Figure 11

The analytical methods applied proved that caffeine can be preserved in an amorphous state using an appropriate preparation method (it was not achieved earlier by other technologies). This is feasible if ultra-rapid drying process is performed in the presence of an appropriate polymer matrix in large proportion. However, increasing the caffeine concentration to 50% the product contains crystals even with very rapid drying.

3.5 In vitro release studies

Dissolution tests were performed in order to determine the release profile of the prepared solid dispersions. The observed morphological differences were expected to be reflected in the dissolution curves of the samples, providing flexibility in matching the dissolution to the requirements.

Figure 12

One can observe comparing the release profiles of the samples presented in Figure 12 that the PLGA, containing hydrophilic as well as hydrophobic units, delayed dissolution of the (highly water soluble) caffeine only slightly. Generally three hours was required to get the total amount of drug dissolved with the exception of the SD_PLGA5 sample, in which case 12 hours was required to evenly dissolve the 5% caffeine. The dissolution profiles of PLA microspheres and fibers are shown in Figure 13 which allows the comparison of the kinetics of their dissolution. As expected, the more hydrophobic PLA biopolymer released the caffeine slower than PLGA, but the difference is moderate in the case of samples containing 50% mainly crystalline drug, in which case the release started with a burst effect, then it slowed down. The rapid dissolution occurs through the channels caused by larger crystals, while the slow release is diffusion controlled. The burst effect was avoided in the case of samples containing the caffeine in amorphous form, which, in agreement with our objectives, provided gradual, slow release. Amorphous substances are, in principle, rapidly soluble, however, in the present case the steady and prolonged dissolution curves can be explained by the fact that the amorphous drug is well dispersed in the polymer matrices.

Figure 13

The results make clear that the release kinetics of both solvent-based processes is highly dependent on the concentration, morphology and distribution of the drug, the duration of the

drying, and the hydrophobicity of the matrix material. In the present case the electrospun product released the drug slower from ES_PLA50 sample than from the relevant spray-dried sample. (Note the dissolution tests were made in aqueous medium and the polymers are not water soluble.) For the two strongly retarded formulations (ES_PLA10 and SD_PLA5 samples) the complete dissolution profile is presented in Figure 13B showing that the time needed for dissolving the total amount of the caffeine is two weeks for SD_PLA5 and as much as four weeks for ES_PLA10. Furthermore, the kinetics of dissolution from ES_PLA10 is close to the most preferred zero order one. The fact that the total dissolution of API is slower from ES_PLA10 than from SD_PLA5 suggests that caffeine forms more homogeneous distribution in the fibers. These assumptions was tried to confirm by Raman mapping.

3.6 Raman mapping

It was assumed that the differences in the dissolution profiles were caused by differences in distribution of API as a consequence of partial phase separation

Figure 14

Comparison of the three images suggests clear differences in the local intensity of the active substance. It is caused by the different spatial distribution within the polymer matrix. The inhomogeneity of API distribution in Figure 14A and 14B is obvious, while in 14C homogeneous distribution can be seen. In the case of SD_PLA10 and SD_PLA5 samples, the phase separation of API and the subsequent crystallization is not prevented (see in Figure 14), while the reason for the preferred gradual sustained release from ES_PLA10 is the perfect, probably molecular, distribution of the drug in the polymer matrix without any sign of crystalline organization.

4. Conclusion

Both continuous technologies of spray drying and electrostatic spinning made it possible to prepare sustained release bioresorbable drug delivery system containing highly water soluble caffeine model drug. Production of microparticles with spray drying, using PLA and PLGA matrices loaded with caffeine, could be performed with high yield. The structure of spray dried particle contains, however, phase separated drug, which tends to crystallize. SD technique requires elevated temperature that is not harmful for caffeine but can damage other thermally unstable compounds. In the case of electrostatic spinning the polymer solution is not exposed to any heat effect and the formed nonwoven structure is easy to handle fitting well to further steps of continuous pharmaceutical production. Using electrostatic spinning it proved to be possible to produce very fine dispersion of caffeine (probably solid solution) at room temperature in PLA matrix when the API content is not higher than 10%. Since caffeine could be amorphized perfectly the burst effect could be avoided and the preferred near to zero order dissolution profile could be ensured. Both technologies are useful in drug delivery systems and their selection depends on the required release profile and on the availability of the facilities. While SD is well developed, the scaling-up of ES in pharmaceutically approved way means some challenges yet. The formed microparticles and nanofibers (in milled form for instance) can be used in subcutaneous injection with controlled drug release.

Acknowledgements

The research was supported by the OTKA Research Fund (code 82426 and code 108975). Besides this project is supported by the New Széchenyi Plan (Project ID: TÁMOP-4.2.1/B-09/1/KMR-2010-0002).

References

[1] Ghosal K, Latha MS, Thomas S. Poly(ester amides) (PEAs) – Scaffold for tissue engineering applications. Eur Polym J 2014;60:58–68. doi:10.1016/j.eurpolymj.2014.08.006.

[2] Mu L, Feng SS. Fabrication, characterization and in vitro release of paclitaxel (Taxol®) loaded poly (lactic-co-glycolic acid) microspheres prepared by spray drying technique with lipid/cholesterol emulsifiers. J Control Release 2001;76:239–54. doi:10.1016/S0168-3659(01)00440-0.

[3] Fu Y-J, Shyu S-S, Su F-H, Yu P-C. Development of biodegradable co-poly(D,L-lactic/glycolic acid) microspheres for the controlled release of 5-FU by the spray drying method. Colloids Surf, B 2002;25:269–79. doi:10.1016/S0927-7765(01)00205-3.

[4] Jiang H, Wang L, Zhu K. Coaxial electrospinning for encapsulation and controlled release of fragile water-soluble bioactive agents. J Control Release 2014;193:296–303. doi:10.1016/j.jconrel.2014.04.025.

[5] Liu W, Wei J, Huo P, Lu Y, Chen Y, Wei Y. Controlled release of brefeldin A from electrospun PEG-PLLA nanofibers and their in vitro antitumor activity against HepG2 cells. Mater Sci Eng C Mater Biol Appl 2013;33:2513–8. doi:10.1016/j.msec.2013.02.013.

[6] Wan F, Maltesen MJ, Andersen SK, Bjerregaard S, Foged C, Rantanen J, et al. One-step production of protein-loaded PLGA microparticles via spray drying using 3-fluid nozzle. Pharm Res 2014;31:1967–77. doi:10.1007/s11095-014-1299-1.

[7] Waeckerle-Men Y, Groettrup M. PLGA microspheres for improved antigen delivery to dendritic cells as cellular vaccines. Adv Drug Deliv Rev 2005;57:475–82. doi:10.1016/j.addr.2004.09.007.

[8] Jain RA. The manufacturing techniques of various drug loaded biodegradable poly (lactide- co -glycolide) (PLGA) devices. Biomaterials 2000;21:2475–90. doi:10.1016/S0142-9612(00)00115-0.

[9] Nagy ZK, Balogh A, Vajna B, Farkas A, Marosi G. Comparison of Electrospun and Extruded Soluplus®-Based Solid Dosage Forms of Improved Dissolution. J Pharm Sci 2012;101:322–32. doi:10.1002/jps.22731.

[10] Bhardwaj N, Kundu SC. Electrospinning: a fascinating fiber fabrication technique. Biotechnol Adv 2010;28:325–47. doi:10.1016/j.biotechadv.2010.01.004.

[11] Tajber L, Corrigan DO, Corrigan OI, Healy a M. Spray drying of budesonide, formoterol fumarate and their composites--I. Physicochemical characterisation. Int J Pharm 2009;367:79–85. doi:10.1016/j.ijpharm.2008.09.030.

[12] Niazi MBK, Zijlstra M, Broekhuis A a. Spray drying thermoplastic starch formulations: Need for processing aids and plasticizers? Eur Polym J 2013;49:1861–70. doi:10.1016/j.eurpolymj.2013.04.016.

[13] Johansen P, Merkle HP, Gander B. Technological considerations related to the up-scaling of protein microencapsulation by spray-drying. Eur J Pharm Biopharm 2000;50:413–7. doi:10.1016/S0939-6411(00)00123-5.

[14] Lasprilla AJR, Martinez G a R, Lunelli BH, Jardini AL, Filho RM. Poly-lactic acid synthesis for application in biomedical devices - a review. Biotechnol Adv 2012;30:321–8. doi:10.1016/j.biotechadv.2011.06.019.

[15] Chen G, Ushida T, Tateishi T. Development of biodegradable porous scaffolds for tissue engineering. Mater Sci Eng C 2001;17:63–9. doi:10.1016/S0928-4931(01)00338-1.

[16] Amalorpava Mary L. Centrifugal spun ultrafine fibrous web as a potential drug delivery vehicle. Express Polym Lett 2013;7:238–48. doi:10.3144/expresspolymlett.2013.22.

[17] Milallos RG, Alexander K, Riga A. Investigation of the interaction between acidic, basic, neutral, and zwitterionic drugs with poly-L-lactic acid by thermal and analytical methods. J Therm Anal Calorim 2008;93:289–94. doi:10.1007/s10973-007-8836-7.

[18] Sacchetti C, Artusi M, Santi P, Colombo P. Caffeine microparticles for nasal administration obtained by spray drying. Int J Pharm 2002;242:335–9. doi:10.1016/S0378-5173(02)00177-1.

[19] Xu J, Jiao Y, Shao X, Zhou C. Controlled dual release of hydrophobic and hydrophilic drugs from electrospun poly(l-lactic acid) fiber mats loaded with chitosan microspheres. Mater Lett 2011;65:2800–3. doi:10.1016/j.matlet.2011.06.018.

[20] Wang J, Wang BM, Schwendeman SP. Mechanistic evaluation of the glucose-induced reduction in initial burst release of octreotide acetate from poly(d,l-lactide-co-glycolide) microspheres. Biomaterials 2004;25:1919–27. doi:10.1016/j.biomaterials.2003.08.019.

[21] Pataki H, Markovits I, Vajna B, Nagy ZK, Marosi G. In-Line Monitoring of Carvedilol Crystallization Using Raman Spectroscopy. Cryst Growth Des 2012;12:5621–8. doi:10.1021/cg301135z.

[22] Paul G, Bruce R. K. Partial least-squares regression: a tutorial. Anal Chim Acta 1986;185:1–17. doi:10.1016/0003-2670(86)80028-9.

[23] Jestel NL. Raman Spectroscopy. In: Bakeev KA, editor. Process Anal. Technol. Second, Oxford, UK: John Wiley & Sons, Ltd; 2010, p. 195–231. doi:10.1002/9780470988459.

[24] Edwards HGM, Lawson E, de Matas M, Shields L, York P. Metamorphosis of caffeine hydrate and anhydrous caffeine. J Chem Soc Perkin Trans 2 1997;9:1985–90. doi:10.1039/A702041D.

[25] Ryder AG, O'Connor GM, Glynn TJ. Quantitative analysis of cocaine in solid mixtures using Raman spectroscopy and chemometric methods . J Raman Spectrosc 2000;31:221–7. doi:10.1002/(SICI)1097-4555(200003)31.

[26] Kister G, Cassanas G, Vert M. Effects of morphology, conformation and configuration on the IR and Raman spectra of various poly(lactic acid)s. Polymer (Guildf) 1998;39:267–73. doi:10.1016/S0032-3861(97)00229-2.

[27] Hubert S, Briancon S, Hedoux A, Guinet Y, Paccou L, Fessi H, et al. Process induced transformations during tablet manufacturing: phase transition analysis of caffeine using DSC and low frequency micro-Raman spectroscopy. Int J Pharm 2011;420:76–83. doi:10.1016/j.ijpharm.2011.08.028.

Figure Captions

Figure 1 Structures of the used drug and polymers in this study: PLGA (A); caffeine (B); PLA (C)

Figure 2 Raman spectra of spray dried caffeine-PLGA solid colloidal dispersion: SD_CAF (A); SD_PLGA80 (B); SD_PLGA60 (C); SD_PLGA50 (D); SD_PLGA40 (E); SD_PLGA30 (F); SD_PLGA25 (G); SD_PLGA20 (H); SD_PLGA10 (I); SD_PLGA5 (J); SD_PLGA (K)

Figure 3 Raman spectra of spray dried and electrospun caffeine-PLA systems: SD_PLA80 (A); ES_PLA50 (B); SD_PLA50 (C); SD_PLA20 (D); ES_PLA10 (E); SD_PLA10 (F); SD_PLA5 (G); SD_PLA (H)

Figure 4 Comparison of PLS regression models regarding PLGA-caffeine (A) and PLA-caffeine (B) systems

Figure 5 SEM images of caffeine loading spray dried and electrospun PLA: SD_PLA (A); ES_PLA (B); SD_PLA10 (C); ES_PLA10 (D); SD_PLA50 (E) and ES_PLA50 (F)

Figure 6 PM images of electrospun PLA with caffeine loading (magnification 100×): ES_PLA50 (A); ES_PLA10 (B)

Figure 7 DSC curves of original PLA (A); original caffeine (B); SD_PLA50 (C); ES_PLA50 (D); SD_PLA10 (E); ES_PLA10 (F); SD_PLA (G) and ES_PLA (H)

Figure 8 DSC curves of original PLGA (A); SD_PLGA80 (B); SD_PLGA60 (C); SD_PLGA50 (D); SD_PLGA40 (E); SD_PLGA30 (F); SD_PLGA10 (G); SD_PLGA5 (H) and SD_PLGA (I)

Figure 9 Enthalpy of the endothermic peak of caffeine melting in PLGA (●) and PLA SD (▲) samples

Figure 10 X-ray diffractogram of caffeine and caffeine loaded PLGA microparticles: original caffeine (A); SD_PLGA60 (B); SD_PLGA50 (C); SD_PLGA40 (D); SD_PLGA30 (E); SD_PLGA25 (F); SD_PLGA20 (G); SD_PLGA10 (H); SD_PLGA5 (I); SD_PLGA (J)

Figure 11 X-ray diffractogram of spray dried and electrospun samples: SD_PLA80 (A); SD_PLA50 (B); SD_PLA20 (C); SD_PLA10 (D); SD_PLA5 (E); ES_PLA50 (F); ES_PLA20 (G); ES_PLA10 (H); SD_PLA (I) and original PLA (J)

Figure 12 Release profiles of caffeine loaded PLGA microspheres

Figure 13 Release profiles of PLA microspheres and fibers loaded with caffeine (A) and total dissolution of SD_PLA5 and ES_PLA10 (B)

Figure 14 Raman maps of the SD_PLA10 (A); SD_PLA5 (B) and ES_PLA10 (C), color code: from black (0.00) to yellow (0.50) for the API spectral concentration

Tables

Table 1 The composition of spray dried microparticles and electrospun samples

Sample code	Caffeine (w/w %)	PLA (w/w %)	PLGA (w/w %)	Yield (%)
SD_PLA80	80	20	-	79
SD_PLA50	50	50	-	74
SD_PLA20	20	80	-	54
SD_PLA10	10	90	-	54
SD_PLA5	5	95	-	72
SD_PLA	0	100	-	76
SD_CAF	100	-	-	65
SD_PLGA80	80	-	20	69
SD_PLGA60	60	-	40	72
SD_PLGA50	50	-	50	76
SD_PLGA40	40		60	62
SD_PLGA30	30		70	67
SD_PLGA25	25		75	68
SD_PLGA20	20		80	63
SD_PLGA10	10	-	90	48
SD_PLGA5	5	-	95	35
SD_PLGA	0	-	100	46
ES_PLA50	50	50	-	97
ES_PLA20	20	80	-	95
ES_PLA10	10	90	-	95
ES_PLA	0	100	-	94

Table 2 Results of regression regarding the PLGA-caffeine and PLA-caffeine systems

Regression method	R^2_C	R^2_{CV}	R^2_{pred}	RMSEC (m/m%)	RMSECV (m/m%)	RMSEP (m/m%)
PLGA-caffeine						
PLS	0.978	0.970	0.974	4.83	6.17	6.28
PLA-caffeine						
PLS	0.957	0.892	0.958	6.61	10.59	4.60

Table 3 Diameter of electrospun PLA fibers prepared from solutions with different polymer concentrations

Table 3

Entry	Samples	Polymer concentration (w/w %)[a]	Polymer: caffeine	Fiber diameter (nm)[b]
1	ES_PLA	10	-	2346±718
2	ES_PLA	6	-	2038±723
3	ES_PLA	4	-	817±172
4	ES_PLA50	4	1:1	1012±367
5	ES_PLA20	4	4:1	996±362
6	ES_PLA10	4	10:1	971±358

[a] The PLA concentration in the solvent mixture

[b] The average fiber diameter and standard deviation was obtained by measuring the size of 200 individual fibers.

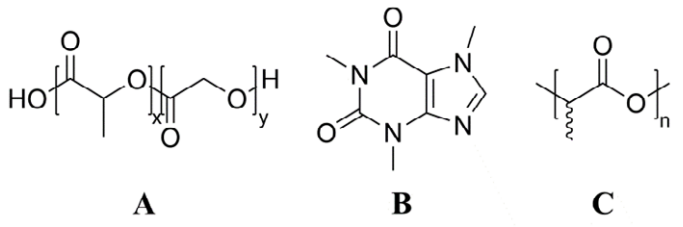
A
B
C

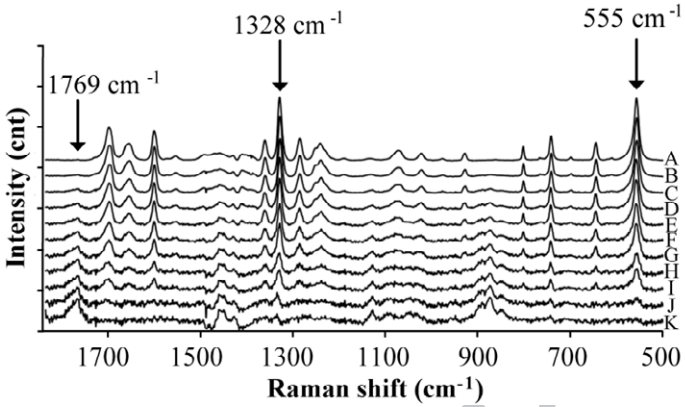
1328 cm -1
555 cm -1
1769 cm -1
Intensity (cnt)
A
B
C
D
E
F
G
H
I
J
K
1700
1500
1300
1100
900
700
500
Raman shift (cm-1)

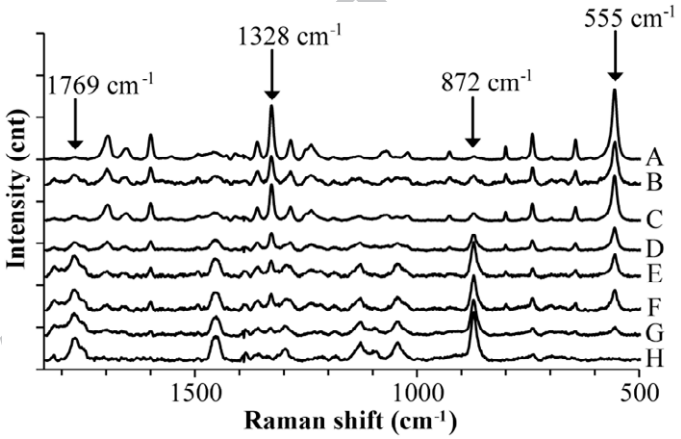
555 cm-1
1328 cm-1
1769 cm-1
872 cm-1
Intensity (cnt)
A
B
C
D
E
F
G
H
1500
1000
500
Raman shift (cm-1)

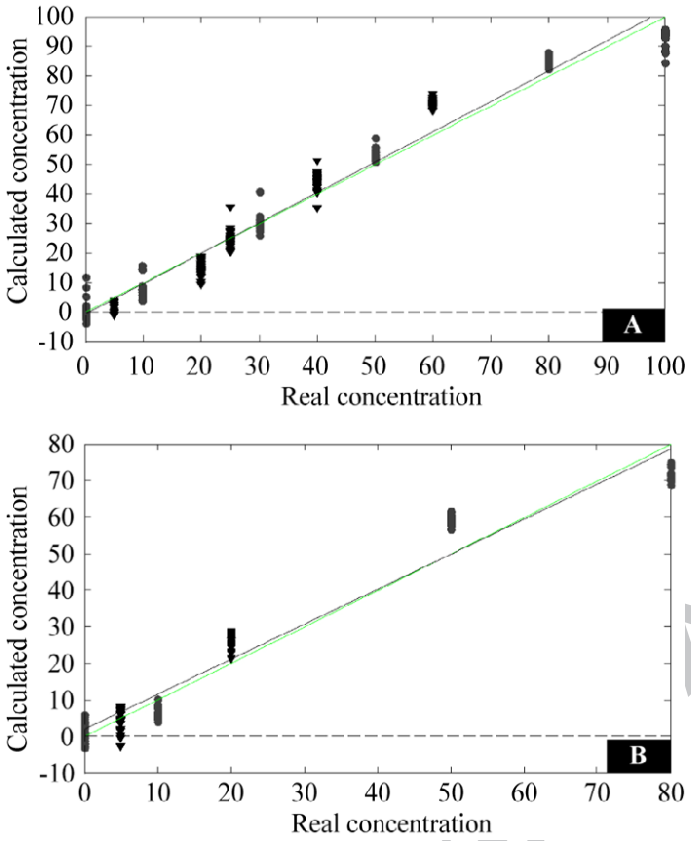

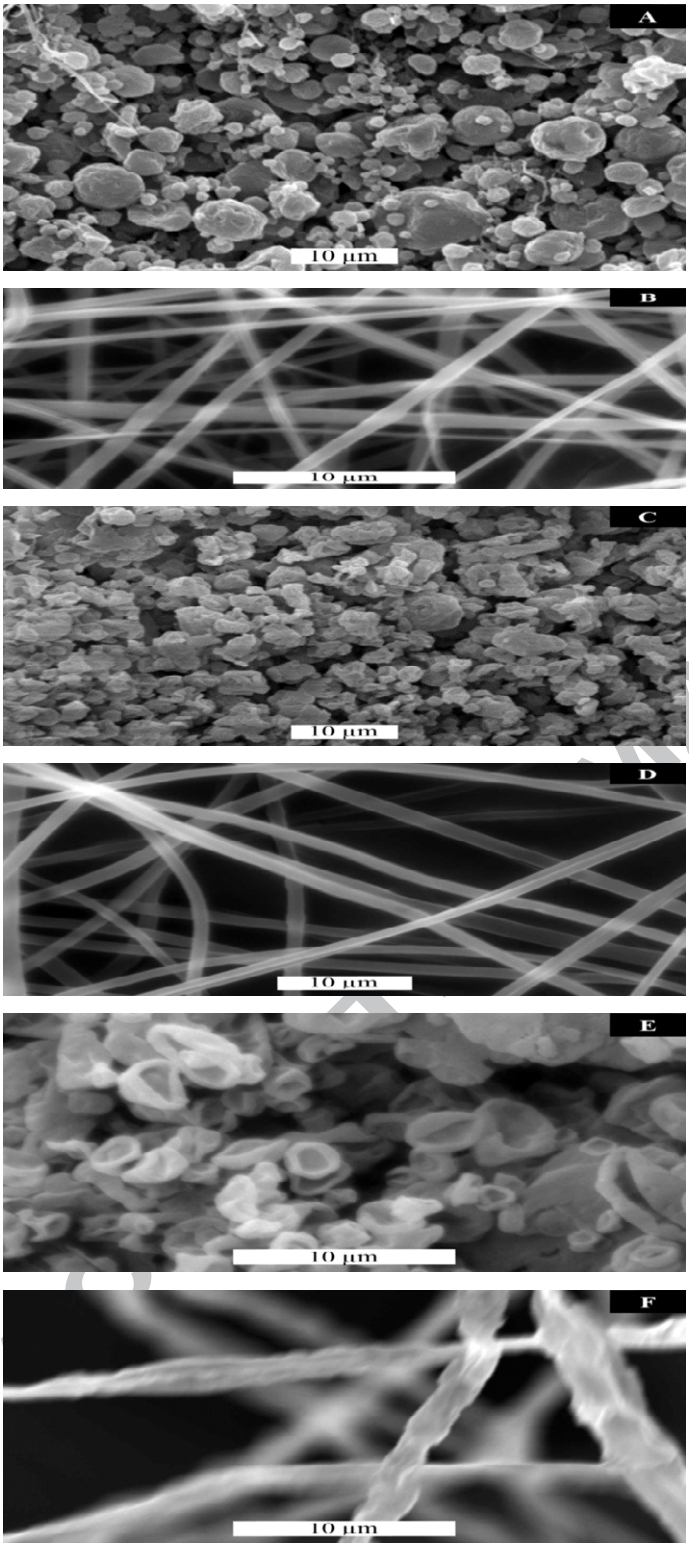

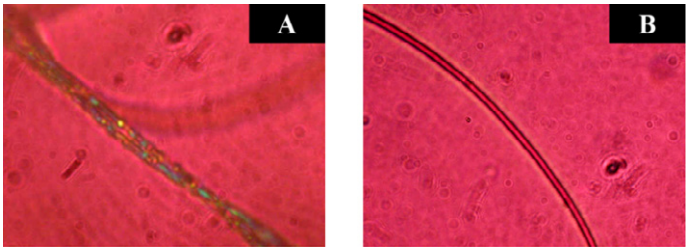

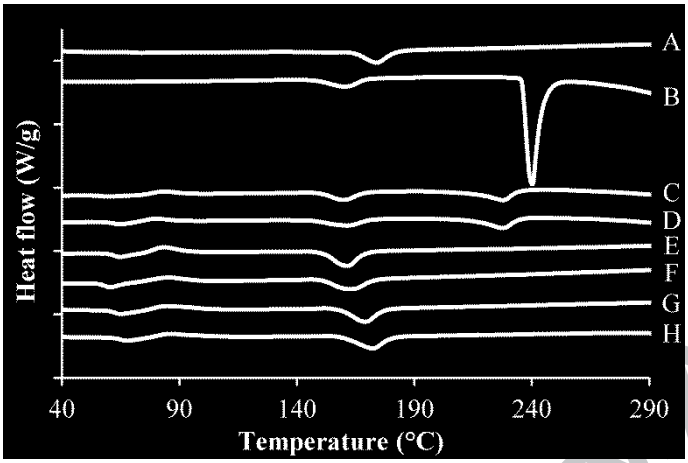

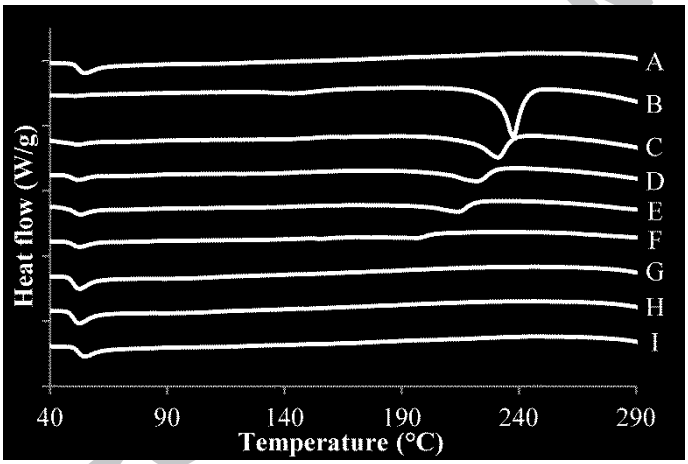

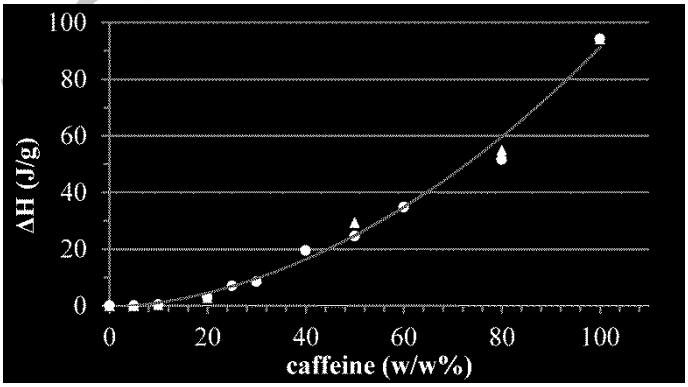

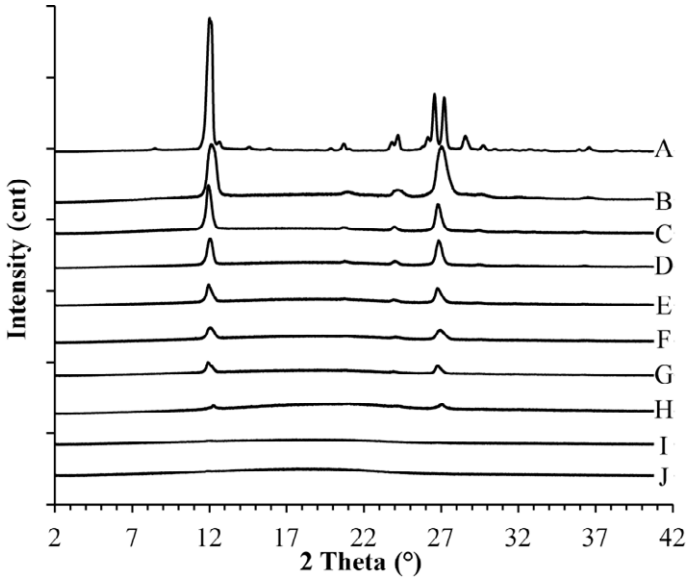
Intensity (cnt)
A
B
C
D
E
F
G
H
I
J
2
7
12
17
22
27
32
37
42
2 Theta (°)

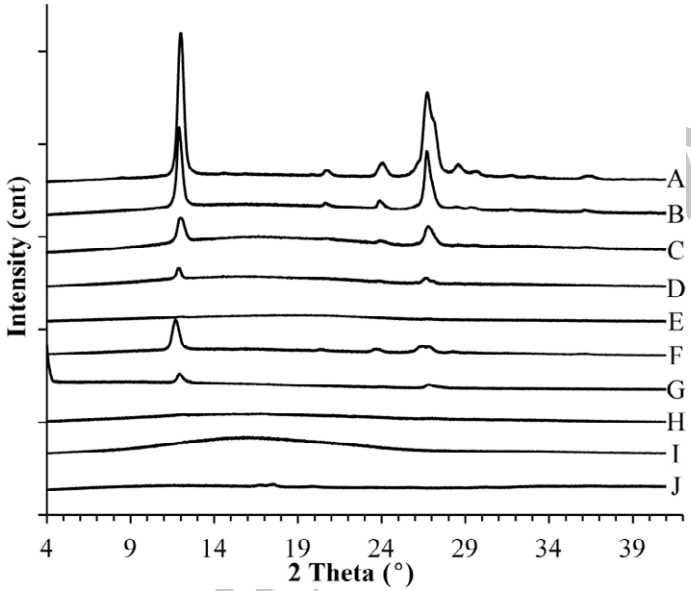
Intensity (cnt)
A
B
C
D
E
F
G
H
I
J
4
9
14
19
24
29
34
39
2 Theta (°)

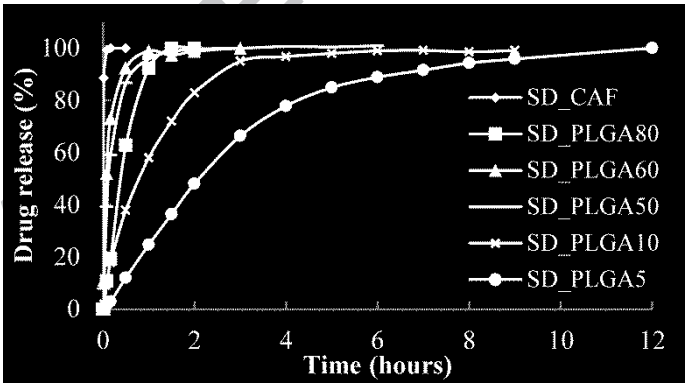
Drug release (%)
100
80
60
40
20
0
SD_CAF
SD_PLGA80
SD_PLGA60
SD_PLGA50
SD_PLGA10
SD_PLGA5
0
2
4
6
8
10
12
Time (hours)

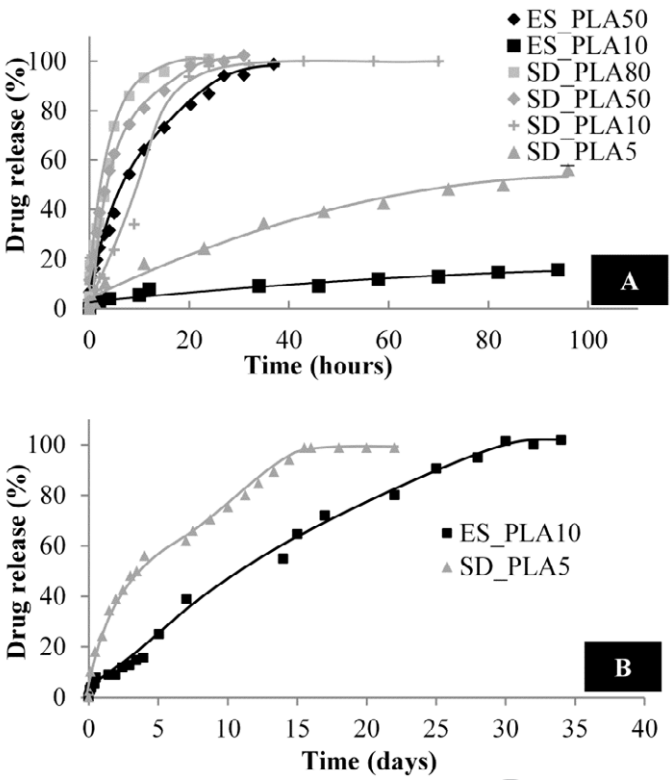

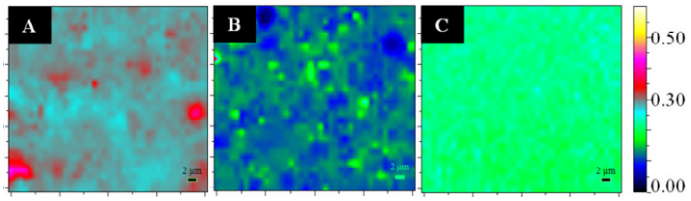

Graphical abstract

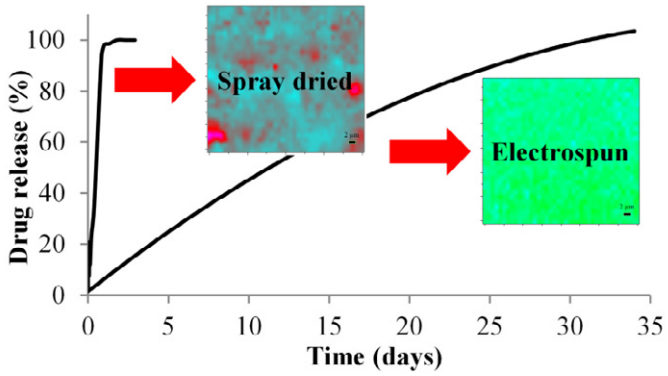

Highlights of the submitted manuscript:

- Raman spectrometry as a potential process analytical technology tool for spray drying
- Spray dried and electrospun bioresorbable drug delivery systems
- Electrospun solid solution for smooth release of water soluble drug